

Nonlinear optical properties of Au₂₅ nanocluster oligomers linked by bidentate dithiol – SUPPORTING INFORMATION

Patryk Obstarczyk^a, Julia Osmólska^a, Michał Swierczewski^b, Thomas Bürgi^b, Marek Samoć^a, and Joanna Olesiak-Bańska^{a*}

^aInstitute of Advanced Materials, Wrocław University of Science and Technology, Wybrzeże Wyspiańskiego 27, 50-370 Wrocław, Poland.

^bDepartment of Physical Chemistry, University of Geneva, 30 Quai Ernest-Ansermet, 1211 Geneva 4, Switzerland.

Experimental section

Materials

All materials were used as purchased, without additional purification steps. Sodium borohydride (≥98.0%, NaBH₄), tetrachloroauric(III) acid (99,9%, HAuCl₄ x 3 H₂O), tetraoctylammonium bromide (98%, TOABr) and HPLC-grade solvents (tetrahydrofuran, toluene, dichloromethane) were sourced from Merck. The SEC column stationary phase (SX1 BioBeds) was bought from Bio-Rads.

Gold nanoclusters synthesis

Gold nanoclusters (monomers, dimers and trimers) were synthesized according to the protocol described by Swierczewski *et al.*¹. In short, [Au₂₅(PET)₁₈]⁰ clusters were prepared by NaBH₄ (0.917g, 50 mL aqueous) mediated reduction of HAuCl₄ x 3 H₂O (1g), TOABr (1.641 g) mixture in THF. The product of the reaction, after two days of aging, was dried under a rotary evaporator and subsequently washed with methanol to remove free thiols. The resulting powder (containing [Au₂₅(PET)₁₈]⁻¹[TOA]⁺) was dissolved in minimal amount of toluene and passed through a SEC column (stationary phase: SX1 BioBeads, Bio-Rad). After that, chosen fractions with [Au₂₅(PET)₁₈]⁻¹[TOA]⁺ (based on UV-Vis spectra) were oxidized over a silica column in dichloromethane. Neutral [Au₂₅(PET)₁₈]⁰ was collected and subsequently purified over a second SEC column. To obtain multimers diBINAS linker was used and ligand exchange reaction was conducted. In brief, 5 mg of [Au₂₅(PET)₁₈]⁰ was dissolved in DCM alongside 0.48 mg of DIBINAS (1:3 ratio) and left mildly stirred under N₂ for 24h at room temperature. The reaction product was dried under rotavapor, dissolved in small amount of DCM and passed through a SEC column, where narrow fractions were collected and analyzed using a Varian Cary 5000 spectrophotometer and MALDI-TOF mass spectrometry.

Linear and nonlinear (z-scan) optical properties measurements

A Jasco V-670 spectrophotometer was utilized to measure the absorption spectra of gold nanoclusters toluene solutions, placed in glass cuvettes: StarnaScientific, path length: 10 mm.

The corresponding gold nanoclusters were re-dissolved in toluene and placed in the thin cuvettes (StarnaScientific, path length: 1 mm). To perform the nonlinear optical properties characterization the z-scan technique was employed. In detail, the closed and open aperture curves (CA, OA, respectively) were measured simultaneously as a function of position along the z axis (corresponding to the propagation direction of a laser beam focused by a lens) of the sample placed on a stage which was moved in the range z=-30 to 30 mm where the focal point of the lens corresponded to z = 0. Three Si or InGaAs photodetectors were utilized (ThorLabs Inc.) for the 600 – 900 and 900 – 1450 nm ranges, respectively for CA, OA and a

reference (the intensity of incident light monitored with a beam splitter before the lens). The photodiode signals were fed into a National Instruments PCI-6143 Multifunction I/O Device and transferred to a computer. The employed laser system was a Coherent Ti: Sapphire Astrella regenerative amplifier combined with an OPA TOPAS Prime (Coherent) optical parametric amplifier providing tunable ~ 60 fs pulses at 1 kHz. The laser power output was attenuated with a polarizer – halfwave plate combination and neutral density filters to obtain intensities in the range from 10 to 300 GW/cm² at the focal point. To take into account the contribution of the solvent, a cuvette with toluene was measured for each corresponding wavelength (Fig. S2) along with those of the solutions and a measurement of CA Z-scan on a fused silica plate served as a way to calibrate the system²⁻³. For the fused silica plate we assume that the nonlinear refractive index can be approximated by the equation

$$n_{2,\text{silica}} = 2.8203 \times 10^{-16} - 3 \times 10^{-21}\bar{\nu} + 2 \times 10^{-25}\bar{\nu}^2 \quad (\text{cm}^2/\text{W})$$

where $\bar{\nu} = 1/\lambda$ is the wavenumber (cm⁻¹), which is a fit to the n_2 data given by Milam⁴. This equation is a good approximation for values of $n_{2,\text{silica}}$ in the range of $\lambda = 500 - 1500$ nm and can be used to determine the light intensity at the focal point from a CA trace obtained on the reference silica plate.

Overall, the collected data were analyzed with a custom-written MatLab script (see our previous works⁵⁻⁶), according to the theory developed by Sheik-Bahae et al.⁷. In detail, since the investigated samples are typically solutions placed in glass cuvettes, to account for the contribution of the solvent and the glass walls of the cuvette we perform the measurements for the cuvette filled with the solvent alone. Typically, such a sample does not show nonlinear absorption in most of the spectral ranges, but its nonlinear refraction often dominates over the contribution coming from the solute. The CA and OA curves for a sample and respective solvent are obtained under the same conditions as in the silica measurement. In general, both the real and imaginary components of the third-order susceptibility of the sample or the second hyperpolarizability (χ) of the solute can then be computed with an assumption that the nonlinear contributions of the solvent and dissolved substance are additive. In the present case the main interest was in the nonlinear absorption which can be quantified assuming that there are two main contributions to it, coming from the two-photon absorption and from saturation of one-photon absorption, as follows:

$$\frac{dI}{dz} = -\alpha(I)I = -\alpha_{SA}I - \alpha_2I^2 \quad (1)$$

$$\text{where:} \quad \alpha_{SA} = \alpha_0 \frac{1}{1 + \frac{I}{I_{sat}}} \quad (2)$$

Fitting of the open aperture Z-scan curves in the case of competition between various processes contributing to nonlinear absorption has been performed using several approaches, the most general being:

- 1) at each position z of the sample in the Z-scan setup the incident light intensity, at the sample front face, i.e. $x = 0$ is calculated as

$$I(z, r, x) = \frac{I_{max}}{1 + \left(\frac{w_0}{w_z}\right)^2} e^{-2\left(\frac{r}{w_z}\right)^2} \quad (3)$$

where I_{max} is the maximum light intensity (determined in a closed-aperture Z-scan experiment performed on a silica plate sample), r is the radial coordinate, w_0 is the focused beam spot radius at the focus ($z = 0$), also determined from the scan performed on silica, w_z is the beam radius at z , given by

$$w_z = w_0 \sqrt{1 + \left(\frac{z}{z_R}\right)^2} \quad (4)$$

where z_R is the Rayleigh length, $z_R = \frac{\pi w_0^2}{\lambda}$.

- 2) Equation (1) is numerically integrated over the thickness of the sample i.e. from $x = 0$ to $x = L$ for all positions of the sample and for concentric rings of the radius r from 0 to the arbitrary limit of $\frac{r}{w_z} = 4$
- 3) The transmittance is calculated at each z as

$$T(z) = \frac{\int_0^{4w_z} r I(z,r,L) dr}{\int_0^{4w_z} r I(z,r,0) dr} \quad (5)$$

The computed curves were compared to the experimental ones, the parameters I_{max} and w_0 being fixed. α_0 was taken to be that obtained from spectrophotometer measurements and essentially equal to the value determined directly in the Z-scan setup by comparing the transmittance of the sample and that of pure solvent at positions far from $z = 0$

Exemplary measurements and calculations results

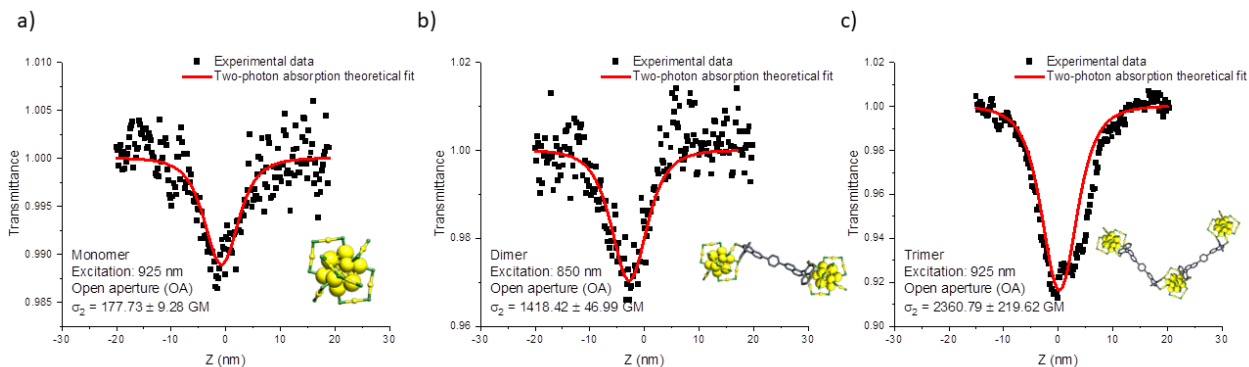


Figure S1. Additional exemplary open-aperture (OA) z-scan traces assigned to two-photon absorption phenomenon, as registered for $[Au_{25}(PET)_{18}]^0$ a) monomer, b) dimer, and c) trimer (linked by bidentate dithiol (diBINAS) and measured in toluene).

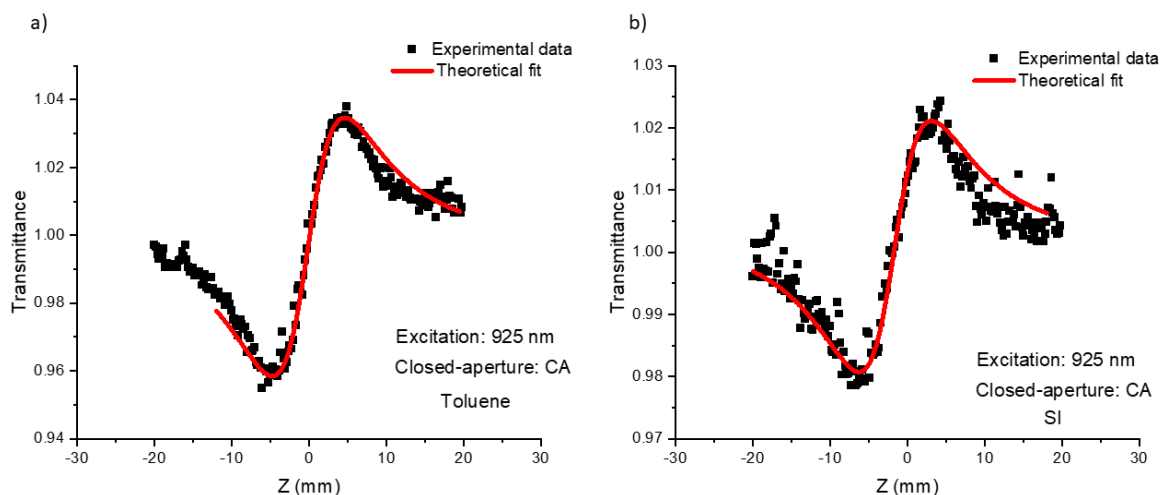


Figure S2. Exemplary closed-aperture (CA) z-scan traces of a) silica (1 mm), and b) toluene. Excitation 925 nm, $w_0 = 40.63 \mu\text{m}$, $I = 18.63 \text{ GW/cm}^2$.

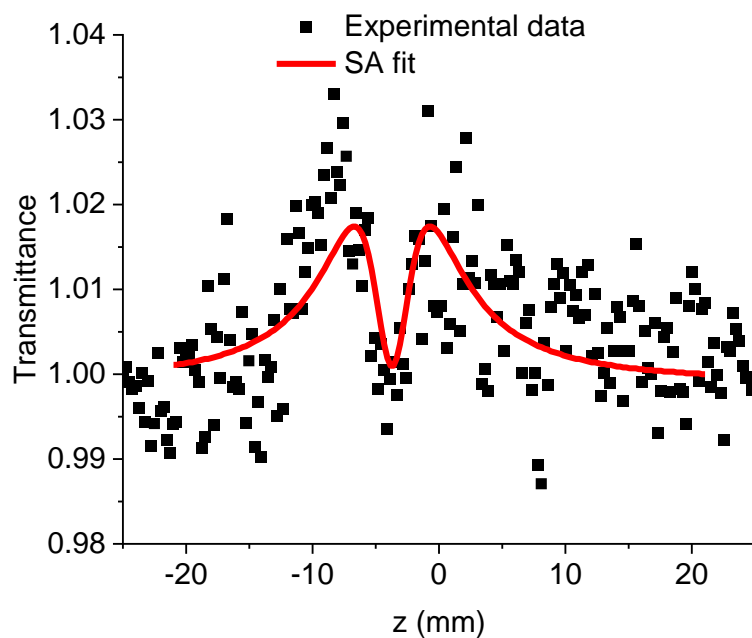


Figure S3. Exemplary open-aperture (OA) z-scan trace assigned to combination of two-photon absorption and saturable absorption phenomenon, as registered for $[\text{Au}_{25}(\text{PET})_{18}]^0$ dimer (linked by bidentate dithiol (diBINAS) and measured in toluene) – 700 nm.

Table S1. One-photon excitation energies, oscillator strengths and 2PA cross sections to 5 lowest excited state for diBINAS in the gas phase computed at the CAM-B3LYP/6-31G** level of theory. Lorentzian broadening was set to 0.2 eV for all excited states. The calculations were performed using GAMESS US program based on the method implemented by Zahariev and Gordon⁸.

Transition	One-photon excitation energy [eV]	Oscillator strength	Two-photon absorption cross section [GM]
$S_0 \rightarrow S_1$	4.086	0.93	<0.1
$S_0 \rightarrow S_2$	4.196	0.07	0.43
$S_0 \rightarrow S_3$	4.307	0.56	0.31
$S_0 \rightarrow S_4$	4.357	0.01	0.54
$S_0 \rightarrow S_5$	4.361	0.09	0.28

Table S2. Overview on two-photon absorption cross sections (σ_2 [GM]) of gold nanoclusters.

Sample	σ_2 [GM]	λ [nm]	Technique	Excitation	Solvent
Au ₂₅ (SR) ₁₈ ⁻¹ Ref. ⁹	2 700	1290	two-photon excited fluorescence	Ti:Sapphire, (100 fs)	hexane
	427 000	800	two-photon excited time-resolved fluorescence up-conversion		
Au ₂₅ (SG) ₁₈ ⁻¹ Ref. ¹⁰⁻¹¹	4.99	755	two-photon excited fluorescence	Ti:sapphire, (140 fs 76 MHz)	water
	189 740	800	z-scan technique	Ti:sapphire, (1 kHz)	water
Au ₂₅ (Capt) ₁₈ ⁻¹ Ref. ⁶	23 000	550	z-scan technique	Ti:sapphire (<130 fs, 1 kHz, 35 – 180 GW/cm ²)	water
	830	800			
	1 510	900			
Au ₂₅ (PET) ₁₈ ⁻¹ Ref. ¹²	$\beta_{\text{eff}} = 2.0 \cdot 10^{-10}$ m/W	532	z-scan technique	Nd:YAG (5 ns, 15 μ J pulse energy)	toluene
L-Arg/ATT-AuNCs Ref. ¹³	1 743 ($\sigma_2^{\text{eff}} = 1102$)	800	two-photon excited fluorescence	Ti:Sapphire (~140 fs, 80 MHz, 22-30 mW)	water
D-Arg/ATT-AuNCs Ref. ¹³	1 453 ($\sigma_2^{\text{eff}} = 848$)				
Au ₈ NCs @ BSA Ref. ¹⁴	537 ($\sigma_2^{\text{eff}} = 5.16$)	740	two-photon-excited fluorescence	Ti:Sapphire (155 fs, 80 MHz)	water
Au ₁₀ (SG) ₁₀ Ref. ¹⁵	10 ($\sigma_2^{\text{eff}} = 0.012$)	800	two-photon excited fluorescence	No data	water

References

1. Swierczewski, M., et al., Exceptionally Stable Dimers and Trimers of Au₂₅ Clusters Linked with a Bidentate Dithiol: Synthesis, Structure and Chirality Study. *Angewandte Chemie International Edition* **2023**, *62*, e202215746.
2. Samoc, M.; Samoc, A.; Dalton, G.; Cifuentes, M.; Humphrey, M.; Fleitz, P., Two-Photon Absorption Spectra and Dispersion of the Complex Cubic Hyperpolarizability γ in Organic and Organometallic Chromophores. 2011; pp 341-355.
3. Samoc, M.; Samoc, A.; Luther-Davies, B.; Humphrey, M. G.; Wong, M.-S., Third-Order Optical Nonlinearities of Oligomers, Dendrimers and Polymers Derived from Solution Z-Scan Studies. *Optical Materials* **2003**, *21*, 485-488.
4. Milam, D., Review and Assessment of Measured Values of the Nonlinear Refractive-Index Coefficient of Fused Silica. *Appl. Opt.* **1998**, *37*, 546-550.
5. Olesiak-Banska, J.; Gordel, M.; Kolkowski, R.; Matczyszyn, K.; Samoc, M., Third-Order Nonlinear Optical Properties of Colloidal Gold Nanorods. *The Journal of Physical Chemistry C* **2012**, *116*, 13731-13737.
6. Olesiak-Banska, J.; Waszkielewicz, M.; Matczyszyn, K.; Samoc, M., A Closer Look at Two-Photon Absorption, Absorption Saturation and Nonlinear Refraction in Gold Nanoclusters. *RSC Advances* **2016**, *6*, 98748-98752.
7. Sheik-Bahae, M.; Said, A. A.; Wei, T. H.; Hagan, D. J.; Stryland, E. W. V., Sensitive Measurement of Optical Nonlinearities Using a Single Beam. *IEEE Journal of Quantum Electronics* **1990**, *26*, 760-769.
8. Zahariev, F.; Gordon, M. S., Nonlinear Response Time-Dependent Density Functional Theory Combined with the Effective Fragment Potential Method. *The Journal of Chemical Physics* **2014**, *140*.
9. Ramakrishna, G.; Varnavski, O.; Kim, J.; Lee, D.; Goodson, T., Quantum-Sized Gold Clusters as Efficient Two-Photon Absorbers. *Journal of the American Chemical Society* **2008**, *130*, 5032-5033.
10. Russier-Antoine, I.; Bertorelle, F.; Vojkovic, M.; Rayane, D.; Salmon, E.; Jonin, C.; Dugourd, P.; Antoine, R.; Brevet, P.-F., Non-Linear Optical Properties of Gold Quantum Clusters. The Smaller the Better. *Nanoscale* **2014**, *6*, 13572-13578.
11. Polavarapu, L.; Manna, M.; Xu, Q.-H., Biocompatible Glutathione Capped Gold Clusters as One- and Two-Photon Excitation Fluorescence Contrast Agents for Live Cells Imaging. *Nanoscale* **2011**, *3*, 429-434.
12. Philip, R.; Chantharasupawong, P.; Qian, H.; Jin, R.; Thomas, J., Evolution of Nonlinear Optical Properties: From Gold Atomic Clusters to Plasmonic Nanocrystals. *Nano Letters* **2012**, *12*, 4661-4667.
13. Pniakowska, A.; Samoć, M.; Olesiak-Bańska, J., Strong Fluorescence-Detected Two-Photon Circular Dichroism of Chiral Gold Nanoclusters. *Nanoscale* **2023**, *15*, 8597-8602.
14. Kindi, H. A.; Mohamed, A.; Kajimoto, S.; Zhanpeisov, N.; Horino, H.; Shibata, Y.; Rzeznicka, I. I.; Fukumura, H., Single Bovine Serum Albumin Molecule Can Hold Plural Blue-Emissive Gold Nanoclusters: A Quantitative Study with Two-Photon Excitation. *Journal of Photochemistry and Photobiology A: Chemistry* **2018**, *357*, 168-174.
15. Bertorelle, F., et al., Au₁₀(Sg)₁₀: A Chiral Gold Catenane Nanocluster with Zero Confined Electrons. Optical Properties and First-Principles Theoretical Analysis. *The Journal of Physical Chemistry Letters* **2017**, *8*, 1979-1985.